ChemComm

Metal-mediated rearrangement of 1,2-diphenylhydrazine to ortho-semidine upon reaction with dichlorotris(triphenylphosphine)ruthenium(II)

Journal:	*ChemComm*
Manuscript ID	CC-COM-08-2022-004500.R1
Article Type:	Communication

COMMUNICATION

Metal-mediated rearrangement of 1,2-diphenylhydrazine to *ortho*-semidine upon reaction with dichlorotris(triphenylphosphine)ruthenium(II)

Received 00th January 20xx,
Accepted 00th January 20xx

DOI: 10.1039/x0xx00000x

Nicolas Cena,[a] Andrew J. Peloquin,[b] Jerry A. Boatz,[c] Sarah Costa,[d] Steven R. Gralinski,[d] Alan L. Balch,[d,*] Kamran B. Ghiassi[c,*]

Reaction between $RuCl_2(PPh_3)_3$, and 1,2-diphenylhydrazine resulted in rearrangement and coordination of *ortho*-semidine. The product, $RuCl_2(PPh_3)_2(\kappa^2\text{-}NH_2\text{-}1,2\text{-}C_6H_4\text{-}NHPh)$, was characterized spectroscopically and the molecular structure was conclusively determined using X-ray crystallography. Computational chemistry was employed to probe the energetics surrounding the rearrangement reaction and product.

Since its discovery over 150 years ago, the rearrangement of 1,2-diphenylhydrazine (hydrazobenzene) remains somewhat of a chemical mystery.[1] The acid-catalysed rearrangement of 1,2-diphenylhydrazine, commonly referred to as the "benzidine rearrangement," results in the production of *para*-benzidine (major), diphenyline (minor), and trace amounts of *ortho*-benzidine, *para*-semidine, and *ortho*-semidine.[2] Rearrangement induced by heat produces the same compounds, but *para*-semidine and *ortho*-semidine reportedly become the major products.[3] The application of thermal energy produces additional decomposition products including hydrogen, azobenzene, and aniline. The different possible rearrangements promoted by acid or heat are illustrated in Scheme 1. Although this arena has been extensively studied, there are only two reports involving transition metal-mediated rearrangements.

In 1995, Davies *et al*. reported the first transition metal-mediated rearrangement of 1,2-diphenylhydrazine producing the square-planar Rh(I) coordination complex, $[Rh(PPh_3)_2(\kappa^2\text{-}NH_2\text{-}1,2\text{-}C_6H_4\text{-}NHPh)]ClO_4$, with a bidentate *ortho*-semidine ligand.[4] The report states that the conversion of 1,2-diphenylhydrazine to *ortho*-semidine is exclusive and catalytic from the starting material, $Rh(PPh_3)_2(nbd)]ClO_4$ (nbd = norbornadiene). Unfortunately, the authors were unable to grow crystals of the coordination compound and determine its solid-state structure conclusively. In 1999, Xia *et al*. detailed the conversion of 1,2-diphenylhydrazine upon reaction with $[(Ph_3P)Au)_3(\mu_3\text{-}O)]BF_4$.[5] In this study, Au(I) mediates the conversion of 1,2-diphenylhydrazine and produces coordination compounds containing the imido ligands of *para*-semidine and *ortho*-semidine in a ratio of 82:18. The crystal structure of the *para* analogue, $[(Ph_3P)Au)_3(\mu_3\text{-}N\text{-}1,4\text{-}C_6H_4\text{-}NHPh)]BF_4$, shows the imido *para*-semidine as bridging between the three Au(I) atoms. Interestingly, the authors note that their observed Au(I)-mediated rearrangements are stoichiometric and not catalytic.

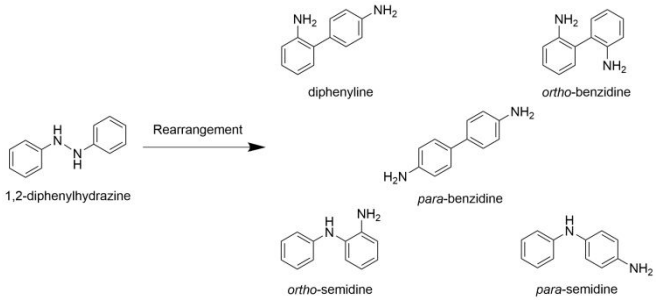

Scheme 1. Rearrangement products of 1,2-diphenylhydrazine.

To our knowledge, there are no reports of 1,2-diphenylhydrazine rearrangements mediated by transition metals for which the formation and coordination of *ortho*-semidine has been crystallographically verified. Expectedly, there are several reports that examined the reactivity between 1,2-diphenylhydrazine and metals.[6] However, rather than rearrangement, the reported compounds stem from N-N bond cleavage or hydrazido ($NHPhNPh^-$) coordination. In addition, there are a few reports with coordinated *ortho*-semidine, though it was the starting material employed.[7]

[a] *HX5, LLC, Air Force Research Laboratory, Aerospace Systems Directorate, Edwards AFB, California 93524, United States.*
[b] *Department of Chemistry and Chemistry Research Center, Laboratories for Advanced Materials, United States Air Force Academy, Colorado Springs, Colorado 80840, United States.*
[c] *Air Force Research Laboratory, Aerospace Systems Directorate, Edwards AFB, California 93524, United States. E-mail: kamran.ghiassi@us.af.mil*
[d] *Department of Chemistry, University of California, Davis, 95616, United States. E-mail: albalch@ucdavis.edu*
Electronic Supplementary Information (ESI) available. See DOI: 10.1039/x0xx00000x

Herein, we report the first crystallographic characterization of the product from rearrangement of 1,2-diphenylhydrazine upon reaction with the prominent catalyst, dichlorotris(triphenylphosphine)ruthenium(II), $RuCl_2(PPh_3)_3$. Hydrazine and some substituted hydrazines have been shown to displace the triphenylphosphine ligands from $RuCl_2(PPh_3)_3$ with the hydrazine acting as a terminal or bridging ligand.[8] However, 1,2-diphenylhydrazine reacts with $RuCl_2(PPh_3)_3$ to produce the chelated compound, $RuCl_2(PPh_3)_2(\kappa^2\text{-}NH_2\text{-}1,2\text{-}C_6H_4\text{-}NHPh)$ (**1**), which involves the transformation of 1,2-diphenylhydrazine to *ortho*-semidine without the occurrence of oxidation-reduction chemistry. No isomerization of 1,2-diphenylhydrazine was observed under similar conditions with triphenylphosphine or with $RuCl_3$ present. Stoichiometric combination of $RuCl_2(PPh_3)_3$ and 1,2-diphenylhydrazine under inert conditions in toluene produced the compound **1**, in 76% yield.[9] The compound contains a bidentate *ortho*-semidine ligand from the rearrangement of 1,2-diphenylhydrazine, as evidenced by X-ray crystallography and NMR spectroscopy. Reaction of $RuCl_2(PPh_3)_3$ and pristine *ortho*-semidine produced the same compound at a slightly lower yield (71%).[9] Both reaction pathways and yields are presented in Scheme 2. Compound **1** is soluble in dichloromethane, chloroform, and toluene and insoluble in diethyl ether, pentane, and hexanes. Solutions of this compound are extremely air-sensitive, turning

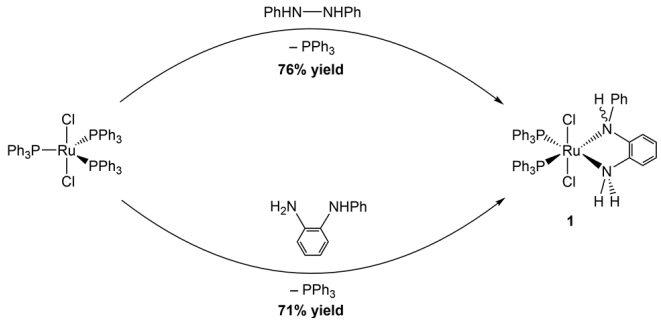

Scheme 2. Synthesis of $RuCl_2(PPh_3)_2(\kappa^2\text{-}NH_2\text{-}1,2\text{-}C_6H_4\text{-}NHPh)$ (**1**) from either 1,2-diphenylhydrazine (top) or *ortho*-semidine (bottom).

purple immediately upon exposure to oxygen. In our hands, we were unable to characterize the oxidized material.

$^{31}P\{^1H\}$ NMR spectroscopy shows that both reactions presented in Scheme 2 result in complete conversion of 1,2-diphenylhydrazine to *ortho*-semidine and formation of compound **1**. Note that upon coordination, one of the nitrogen atoms becomes a chiral centre. The reactions are stoichiometric rather than catalytic, similar to the Au(I)-mediated report.[5] At substoichiometric ratios, both product and $RuCl_2(PPh_3)_3$ starting material are present. When the ratio employed was 1:1 or higher, the $RuCl_2(PPh_3)_3$ is completely consumed resulting solely in the formation of compound **1**. Fig. 1 shows the room temperature $^{31}P\{^1H\}$ NMR spectra at relevant stoichiometric ratios.

Although there are two inequivalent phosphorous positions, the room temperature $^{31}P\{^1H\}$ NMR spectrum presents as a broad singlet at 44.3 ppm due to ligand exchange and fluxionality. Variable temperature $^{31}P\{^1H\}$ NMR was utilized and spectra at relevant temperatures are shown in Fig.

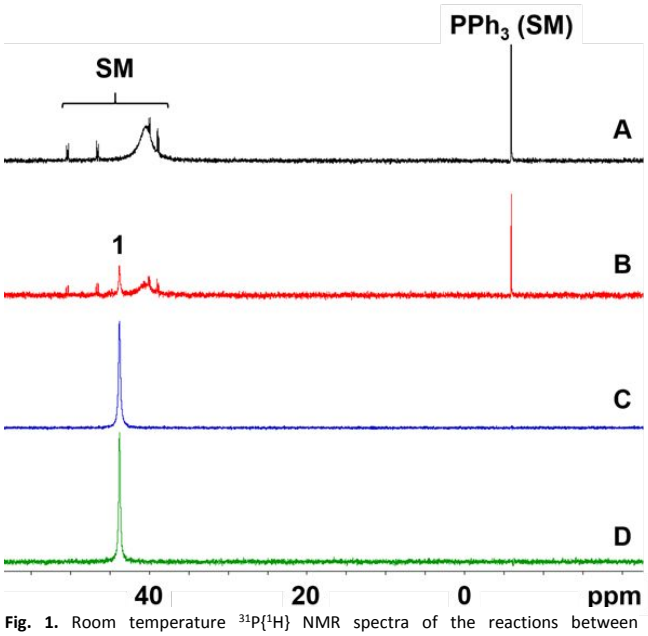

Fig. 1. Room temperature $^{31}P\{^1H\}$ NMR spectra of the reactions between $RuCl_2(PPh_3)_3$ and 1,2-diphenylhydrazine in $CDCl_3$. Trace A shows the starting material (SM) $RuCl_2(PPh_3)_3$ that immediately liberates PPh_3 upon dissolution. Trace B shows the reaction at a 0.5:1 ratio. Trace C shows the reaction at a 1:1 ratio. Trace D shows the reaction of $RuCl_2(PPh_3)_3$ and pristine *ortho*-semidine at a 1:1 ratio.

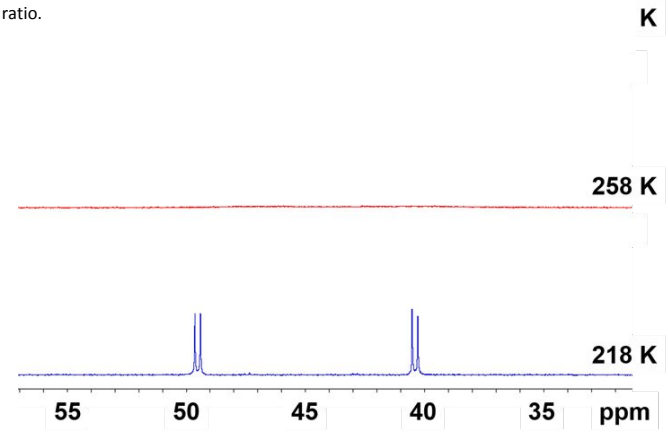

Fig. 2. Variable temperature $^{31}P\{^1H\}$ NMR of $RuCl_2(PPh_3)_2(\kappa^2\text{-}NH_2\text{-}1,2\text{-}C_6H_4\text{-}NHPh)$ (**1**) in $CDCl_3$. Top shows a broad singlet at 44.3 ppm at 298 K. Middle shows the coalescence temperature at 258 K. Bottom shows the resolved doublets at 48.0 ppm ($^2J_{P,P}$ = 37 Hz), and 38.2 ppm ($^2J_{P,P}$ = 37 Hz) at 218 K.

2. The coalescence temperature was determined to be 258 K. The ΔG for this exchange was calculated to be 45.2 kJ mol^{-1} (10.8 kcal mol^{-1}), which is consistent with exchange of the cis equatorial inequivalent phosphines.[10]

Single crystals of compound **1** suitable for X-ray diffraction were obtained by vapour diffusion of pentane into a toluene solution of the compound.[11] Two polymorphs were discovered during the employment of this recrystallization method. Chronologically, the first observed polymorph, designated as ***α*-1**, crystallizes as yellow plates in the monoclinic space group $P2_1/n$ with Z = 4 and Z' = 1. Since the space group is centrosymmetric, the crystal structure is racemic and contains both *R* and *S* enantiomers. The asymmetric unit consists of one hand, with the second enantiomer generated by crystallographic inversion. Across three different laboratories

and research groups, we were unable to obtain this form more than once. The late Professor Joel Bernstein would classify the ***α*-1** form as a "disappearing polymorph" due to its experimental observation, yet inability to be observed again.[12]

Ironically, the most prevalent form, designated as ***β*-1**, was observed last. Crystals of orange plates residing in the chiral space group $P2_12_12_1$ with Z = 4 and Z' = 1 contain the *S* enantiomer. Several crystals were examined; each contained the S enantiomer, though it is probable that the material is a racemic conglomerate. Powder X-ray diffraction (Fig. S9) shows that the bulk crystalline sample is phase pure of the ***β*-1** form; there is no contamination of the ***α*-1** polymorph.[13] Thus, the observation of the ***α*-1** polymorph is most serendipitous and an invitation for future research. The molecular structures of each polymorph are presented in Fig. 3. It is fascinating that compound **1** reproducibly undergoes chiral resolution to yield the prevailing polymorph. It is all the more puzzling (and ironic) that the racemic, centrosymmetric structure, which is far more frequently observed in crystallography, was only observed once. Since both crystal structures are nearly

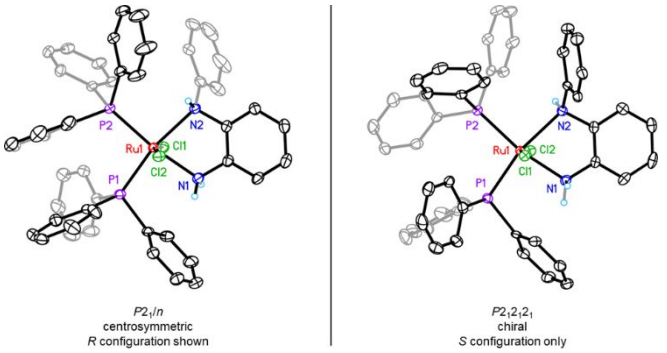

$P2_1/n$
centrosymmetric
R configuration shown

$P2_12_12_1$
chiral
S configuration only

Fig. 3. The molecular components for the ***α*-1** (left) and ***β*-1** (right) structures of $RuCl_2(PPh_3)_2(\kappa^2\text{-}NH_2\text{-}1,2\text{-}C_6H_4\text{-}NHPh)$ (**1**) drawn with 50% thermal contours. Hydrogen positions are omitted for clarity with the exception of the nitrogen atoms. Note that the centrosymmetric $P2_1/n$ structure is racemic, while the chiral $P2_12_12_1$ structure is enantiopure.

identical from the point of view of the metal centre, the remainder of this work will refer to the ***β*-1** form unless otherwise specified.

Compound **1** shows the six-coordinate octahedral ruthenium(II) centre coordinated by two chlorine atoms, two triphenylphosphine groups, and a bidentate *ortho*-semidine. The structure shows that the chlorines are trans (axial) and are angled slightly towards the *ortho*-semidine. The hydrogen atoms on the *ortho*-semidine ligand were found in the difference Fourier map of the X-ray experiment and freely refined. The Ru–N, Ru–P, Ru–Cl bond distances, and all bond angles, are within the expected range. Crystallographic data and relevant bond distances and angles are provided in ESI (Tables S1 and S2, respectively).

To gain further insight into the rearrangement and reactivity processes to form compound **1**, density functional theory (DFT) calculations were performed to predict the gas-phase Gibbs free energies of reaction of the pathways shown in Scheme 2 and Eqs. 1-3 below.[14] As shown in Equations 1 and 2, both pathways to form product **1** are exergonic, thus confirming the thermodynamic favourability of the 1,2-diphenylhydrazine to *ortho*-semidine rearrangement process to form compound **1**. It is curious that although the reactions are quite similar, the rearrangement of 1,2-diphenylhydrazine and subsequent formation of **1** is approximately an order of magnitude more favoured than direct coordination of *ortho*-semidine. Indeed, this increase in favourability is due to the exergonic transformation of 1,2-diphenylhydrazine to *ortho*-semidine shown in Eq. 3.

$RuCl_2(PPh_3)_3$ + PhHN-NHPh → $RuCl_2(PPh_3)_2(\kappa^2\text{-}NH_2\text{-}1,2\text{-}C_6H_4\text{-}NHPh)$ + PPh_3
ΔG = -107 kJ mol^{-1} (Eq. 1)

$RuCl_2(PPh_3)_3$ + NH_2-1,2-C_6H_4-NHPh → $RuCl_2(PPh_3)_2(\kappa^2\text{-}NH_2\text{-}1,2\text{-}C_6H_4\text{-}NHPh)$ + PPh_3
ΔG = -16 kJ mol^{-1} (Eq. 2)

PhHN-NHPh → NH_2-1,2-C_6H_4-NHPh
ΔG = -91 kJ mol^{-1} (Eq. 3)

Not including enantiomers, there are six unique spatial isomers of compound **1**, as illustrated in Fig. 4. The isomers were determined by considering all possible combinations of the chlorine and triphenylphosphine ligands in axial versus equatorial positions, coupled with the orientation of the substituents on the chiral nitrogen centre in the *ortho*-semidine ligand while retaining its bidentate configuration. Fig. S11 shows the predicted structures and free energies. Table S2 in ESI provides the computed bond lengths and angles for the first coordination sphere. As shown in Fig. 4, the five predicted isomers **1b** – **1f** are less stable relative to the experimentally-observed compound **1**, with free energies ranging from +21 to +57 kJ mol^{-1}. The predicted bond distances and angles for compound **1** are in good agreement with the crystal structure data.

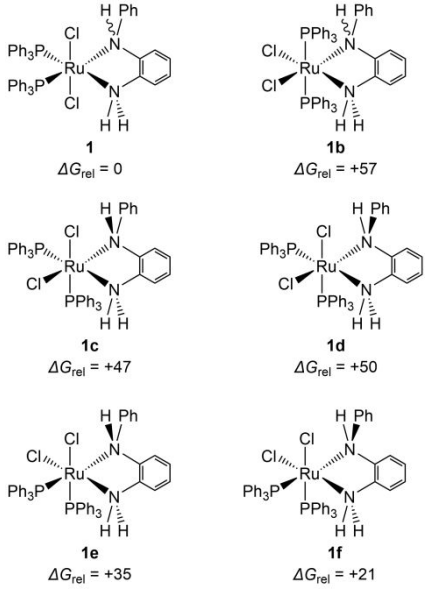

Fig. 4. The unique spatial isomers of $RuCl_2(PPh_3)_2(\kappa^2\text{-}NH_2\text{-}1,2\text{-}C_6H_4\text{-}NHPh)$. Enantiomers are not included. Solvent-corrected (chloroform) Gibbs free energies reported in kJ mol^{-1}. Computational details are provided in ESI.

It should be mentioned that the calculations predict a monodentate structure (**1g**), shown in Fig. 5, as slightly more stable than **1** by 26 kJ mol^{-1}. We speculate that this monodentate species exists in solution at room temperature and is in equilibrium with the bidentate compound **1**, giving rise to the broad singlet observed in the room temperature ^{31}P NMR spectrum (Fig. 2). Crystal packing effects may induce the formation of the bidentate structure in the solid state due to more favourable crystallization enthalpy, while solutions at lower temperature have less available energy needed for ligand lability. Unfortunately, we were unable to isolate the monodentate species **1g** experimentally, nor computationally locate a saddle point connecting the bidentate and monodentate structures to determine the free energy of activation of fluxional ligand interchange.

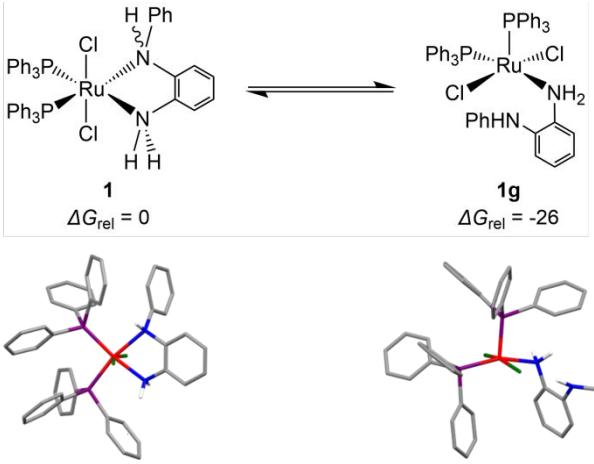

Fig. 5. Top: Proposed room-temperature, solution-based equilibrium of **1** alternating between bidentate and monodentate coordination. Bottom: DFT-predicted structures of **1** and **1g**. Solvent-corrected (chloroform) Gibbs free energies reported in kJ mol^{-1}. Colour code: carbon (grey), hydrogen (white), nitrogen (blue), phosphorus (purple), chlorine (green), ruthenium (red). Phenyl hydrogen atoms are omitted for clarity.

To summarize, since its discovery nearly two centuries ago, the rearrangement of 1,2-diphenylhydrazine is still a source of unique and interesting chemistry. Reaction with $RuCl_2(PPh_3)_3$ provides the first crystallographically-verified report of a transition metal-mediated transformation to *ortho*-semidine. This conversion is exclusively to *ortho*-semidine and proceeds in a stoichiometric fashion. Although computational chemistry provides a unique perspective on the energetic landscape of this particular system, $RuCl_2(PPh_3)_2(\kappa^2\text{-}NH_2\text{-}1,2\text{-}C_6H_4\text{-}NHPh)$ provides its own mystery with the case of a "disappearing polymorph."

The authors are grateful for the financial support of the National Science Foundation Grants CHE-1305125 and CHE-1807637 to A.L.B., the Air Force Office of Scientific Research (AFOSR), and the Aerospace Systems Directorate. This work was supported in part by high-performance computer time and resources from the DoD High Performance Computing Modernization Program. The authors also thank Professor Emeritus Bruce M. Foxman for insightful discussion on this work.

Conflicts of interest

There are no conflicts to declare.

Notes and references

1 A. W. Hoffman, *Proc. R. Soc. London*, 1863, **12**, 576.
2 (*a*) R. B. Carlin, R. G. Nelb and R. C. Odioso, *J. Am. Chem. Soc.*, 1951, **73**, 1002. (*b*) G. S. Hammond and W. Grundemeier, *J. Am. Chem. Soc.*, 1955, **77**, 2444. (*c*) H. J. Shine, in *Aromatic Rearrangement*, Elsevier, New York, 1967, pp. 126–179. (*d*) M. J. S. Dewar, in *Molecular Rearrangement*, ed. P. de Mayo, Interscience, New York, 1969, vol. 1, pp. 323–343. (*e*) H. J. Shine, in *Mechanisms of Molecular Migrations*, ed. B. S. Thyagarajan, Interscience, New York, 1969, vol. 2, pp. 191–247. (*f*) D. V. Banthorp, *Chem. Rev.*, 1970, **70**, 295. (*g*) R. A. Cox and E. Buncel, in *The Chemistry of the Hydrazo, Azo, and Azoxy Groups*, ed. S. Patai, Wiley, New York, 1975, pp. 775–859. (*h*) C. A. Bunton and R. J. Rubin, *J. Am. Chem. Soc.*, 1976, **98**, 4236.
3 (*a*) G. O. Curme, *J. Am. Chem. Soc.*, 1913, **35**, 1143. (*b*) P. F. Holt and B. P. Hughes, *J. Chem. Soc.* 1953, 1666. (*c*) M. Vecera, J. Gasparic and J. Petranek, *Chem. Ind.*, 1957, 299.
4 C. J. Davies, B. T. Heaton and C. Jacob, *J. Chem. Soc., Chem. Commun.*, 1995, 1177.
5 A. Xia, A. J. James and P. R. Sharp, *Organometallics*, 1999, **18**, 451.
6 (*a*) J. M. Carnick, F. A. Cotton, L. R. Falvello and S. A. Duraj, *Inorg. Chim. Acta*, 1988, **143**, 185. (*b*) W. J. Evans, G. Kociok-Kohn, V. S. Leong and J. W. Ziller, *Inorg. Chem*. 1992, **31**, 3592. (*c*) R. R. Schrock, T. E. Glassman, M. G. Vale and M. Kol, *J. Am. Chem. Soc.*, 1993, **115**, 1760. (*d*) C. H. Zambrano, P. R. Sharp and C. L. Barnes, *Organometallics*, 1995, **14**, 3607. (*e*) C. R. Hamilton, M. R. Gau, R. A. Baglia, S. F. McWilliams and M. J. Zdilla, *J. Am. Chem. Soc.* 2014, **136**, 17974.
7 (*a*) A. A. Sidorov, S. A. Deomidov, S. E. Nefedov, I. G. Fomina, P. V. Danilov, V. M. Novotortsev, O. G. Volkov, V. N. Ikorskii and I. L. Eremenko, *Russ. J. Inorg. Chem.* 1999, **44**, 396. (*b*) Sidorov, A. A., Fomina, I. G., Malkov, A. E., Reshetnikov, A. V., Aleksandrov, G. G., Novotortsev, V. M., Nefedov, S. E., Eremenko, I. L. *Russ. Bull. Chem.* 2000, **49**, 1887. (*c*) I. G. Fomina, A. A. Sidorov, G. G. Aleksandrov, V. N. Ikorskii, V. M. Novotortsev, S. E. Nefedov and I. L. Eremenko, *Russ. Bull. Chem.*, 2002, **51**, 1851. (*d*) T. I. A. Gerber, R. Betz, I. N. Booysen, K. C. Potgieter, and P. Mayer, *Polyhedron.* 2011, **30**, 1739.
8 N. Cena, A. J. Peloquin, M. M. Aristov, X. B. Carroll, S. T. Iacono, J. A. Boatz, M. M. Olmstead, A. L. Balch and K. B. Ghiassi, *Polyhedron*, **222**, 115899.
9 Synthesis details for both reactions and characterization data are provided in ESI.
10 (*a*) W. A. Thomas, *Ann. Rep. NMR Spec.* 1968, **1**, 43. (*b*) R. A. Palmer and D. R. Whitcomb, *J. Mag. Reson.* 1969, **39**, 371. (*c*) A. J. Gordon and R. A. Ford, in *The Chemist's Companion: A Handbook of Practical Data, Techniques, and References*, Wiley, New York, 1972.
11 Single-crystal X-ray diffraction experimental details and data are provided in ESI.
12 (*a*) J. D. Dunitz and J. Bernstein, *Acc. Chem. Res.*, 1995, **28**, 193. (*b*) D.-K. Bucar, R. W. Lancaster and J. Bernstein, *Angew. Chem., Int. Ed.*, 2015, **54**, 6972.
13 Powder X-ray diffraction experimental details, experimentally-determined diffractogram, and predicted diffractograms for the ***α*-1** and ***β*-1**polymorphs are provided in ESI.
14 Computational protocol, predicted structures, and coordinates are provided in ESI.